

# Phase-transition-induced residual strain in ferromagnetic MnAs films epitaxially grown on GaAs(001)

A. Trampert,<sup>a)</sup> F. Schippan, L. Däweritz, and K. H. Ploog

Paul-Drude-Institut für Festkörperelektronik, Hausvogteiplatz 5–7, D-10117 Berlin, Germany

(Received 24 October 2000; accepted for publication 23 February 2001)

We investigate the atomic interface structure and the residual strain state of ferromagnetic  $\alpha$  (hexagonal) MnAs layers on cubic GaAs(001) by means of high-resolution transmission electron microscopy and electron diffraction. Despite the different symmetries of the adjacent planes at the heterointerface and the large and orientation-dependent lattice mismatch, the hexagonal MnAs grows epitaxially on GaAs(001) with the  $(1\bar{1}.0)$  prism plane parallel to the cubic substrate. The atomic arrangement at the interface, which is defined by the accommodation of the large lattice mismatch, explains this extreme case of heteroepitaxial alignment. The anisotropic residual strain distribution is discussed with respect to the particular process of lattice misfit relaxation in the presence of the ferromagnetic phase transition. © 2001 American Institute of Physics. [DOI: 10.1063/1.1367302]

The magnetic properties of epitaxial thin layers are strongly correlated to their elastic strain state. For example, residual strain in CrO<sub>2</sub> epilayers has a marked effect on the magnetic anisotropy as a function of film thickness.<sup>1</sup> Moreover, epilayer strain is able to suppress the saturation of the magnetic moment or can shift the Curie temperature  $T_c$  of the ferromagnetic transition as it is found in SrRuO<sub>3</sub>.<sup>2</sup> The exact knowledge of the film strain state is, therefore, a prerequisite for a more-detailed understanding of this anomalous physical behavior in epitaxial magnetic thin films.

In the case of heteroepitaxial growth, the natural strain in the epilayers is a result of the misfit in lattice parameter and thermal expansion coefficient and of the plastic relaxation process. Additionally, this intrinsic natural strain is influenced by a discontinuous volume change at  $T_c$  in materials which show a spontaneous volume magnetostriction. The epitaxial MnAs–GaAs system is regarded as a model system to study the interplay between epitaxy- and phase-transition-induced strain. Hexagonal MnAs on cubic GaAs is an extreme example for heteroepitaxial systems because this material combination has not only a large lattice misfit, but there is also a huge difference in crystal symmetry and bonding character of the adjacent atom planes at the interface. Second, bulk material of MnAs, which is ferromagnetic at room temperature, abruptly loses its magnetization at  $T_c \approx 45^\circ\text{C}$  and simultaneously undergoes a structural transition from the hexagonal  $\alpha$  phase to the orthorhombic  $\beta$  phase.<sup>3</sup> This transition at  $T_c$  is accompanied by an anomalous large discontinuous volume change of  $\Delta V/V \approx 2\%$ , which is caused by a giant spontaneous volume magnetostriction.<sup>4,5</sup>

In this letter, we study the atomic structure of the  $\alpha$ -MnAs/GaAs(001) interface by high-resolution transmission electron microscopy (HRTEM). The interface structure is responsible for the epitaxial alignment, i.e., the orientation relationship between these different crystal lattices and, additionally, it determines the way of lattice mismatch accommodation and strain relief. The residual strain distribution,

which is anisotropic in the thin MnAs epilayers, is measured on a microscopic as well as atomic scale and its origin is discussed in terms of the plastic relaxation processes in connection with the occurrence of the structural phase transition at  $T_c$ .

Thin films of hexagonal MnAs are deposited on cubic GaAs(001) substrates by solid-source molecular-beam epitaxy. A 100-nm-thick GaAs buffer layer is grown in order to realize well-defined substrate surfaces for the following heteroepitaxy. The growth temperature and growth rate of MnAs is about  $250^\circ\text{C}$  and in the range of  $9\text{--}21\text{ nm h}^{-1}$ , respectively.<sup>6</sup> *In situ* reflection high-energy electron diffraction (RHEED) shows the following epitaxial orientation relationship: MnAs  $(1\bar{1}.0) \parallel \text{GaAs}(001)$  and MnAs  $[00.1] \parallel \text{GaAs}[1\bar{1}0]$  [Fig. 1(a)]. For the structural investigations, a series of transmission electron microscopy (TEM) specimens with varying MnAs epilayer thicknesses is prepared using standard techniques involving mechanical grinding, dim-

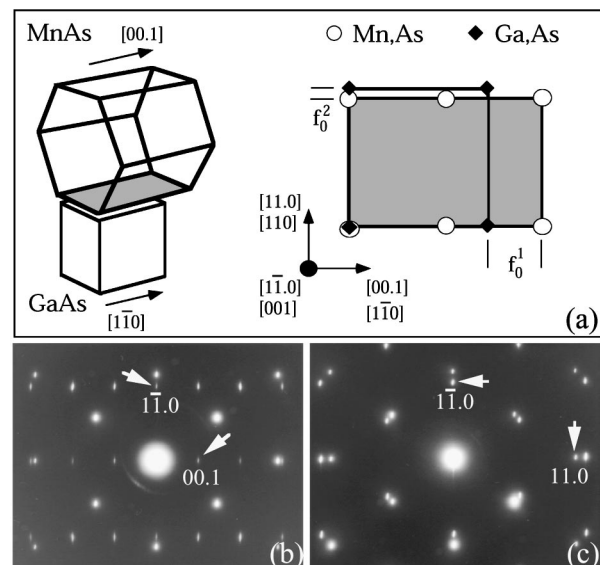


FIG. 1. (a) Schematic illustration of the MnAs/GaAs heterostructure in three dimensions (left) and of the interface in plan view (right); (b) SAD pattern in the cross-sectional direction along GaAs $[110] \parallel \text{MnAs}[11.0]$  and (c) along GaAs $[1\bar{1}0] \parallel \text{MnAs}[00.1]$ .

<sup>a)</sup>Author to whom correspondence should be addressed; electronic mail: trampert@pdi-berlin.de

pling, and Ar-ion-beam milling in a cold stage in order to minimize sample damage. The TEM observations are carried out in the JEM 4000FX and JEM 3010 microscopes.

The crystal structure of the MnAs films appears homogeneous in the TEM, no granular morphology is visible, which would be expected in the presence of orientation or phase variations. Some dislocations are detected near the heteroboundary and within the epilayer originating from the misfit accommodation process. The single-crystalline structure is also verified by electron diffraction measurements. Figures 1(b) and 1(c) show selected area diffraction (SAD) patterns obtained from two different directions with respect to the GaAs substrate: (b) cross-sectional view parallel to the  $[110]$  and (c) parallel to the GaAs  $[1\bar{1}0]$  direction. These SAD patterns confirm the orientation relationship between both crystal lattices obtained by the *in situ* RHEED experiments. The distances between the diffraction spots are measured in order to estimate the lattice parameters of the hexagonal MnAs by using the diffraction spots of GaAs as a calibration standard. Setting  $a_{\text{GaAs}} = 0.565\,325$  nm and selecting the  $[00.4]$  spot in Fig. 1(b), we obtain the MnAs lattice constant  $c = (0.570 \pm 0.004)$  nm, which agrees within the limits of error to the bulk value given in the literature,  $c_{\text{bulk}} = (0.571 \pm 0.002)$  nm.<sup>7</sup> The lattice constant  $a$  is determined from the SAD pattern taken from the perpendicular direction along the  $[00.1]$  zone axis [Fig. 1(c)]. By selecting the  $(11.0)$  spot, i.e., the lattice planes perpendicular to the interface, we obtain the constant  $a_{\parallel} \equiv 2d_{11.0} = (0.369 \pm 0.004)$  nm parallel to the interface. However, if we measure the distance of the lattice planes lying parallel to the interface and corresponding to the  $(1\bar{1}.0)$  reflection, the lattice parameter is determined by  $a_{\perp} \equiv \sqrt{4/3}d_{1\bar{1}.0} = (0.379 \pm 0.004)$  nm, a value which is considerably larger than  $a_{\parallel}$ . Therefore, the SAD measurement points to an anisotropic residual strain state of the epilayers with *compressive* strain along the  $[1\bar{1}.0]$  and almost no strain along the  $[00.1]$  direction. This result will be explained in the following by the asymmetric character of the interface structure and by distinct mechanisms of strain relief, especially in the presence of  $T_c$ .

Generally, the lattice misfit which is defined by  $f^i = (a_o^i - a_s^i)/a_s^i$ ,  $i = 1, 2$  with the unstrained spacings of the corresponding atoms in overlayer  $a_o$  and substrate  $a_s$ , respectively, strongly depends on the inspected in-plane direction  $i$ . In the case of the MnAs/GaAs system [cf. Fig. 1(a)], the lattice misfit  $f^1$  corresponding to the  $[1\bar{1}0]$  GaAs-direction, i.e., between the  $\{00.2\}$  MnAs and the  $\{110\}$  GaAs planes, amounts to 30% if we use the published bulk values for the calculation.<sup>7</sup> The value  $f^2$  for the GaAs  $[110]$  direction, i.e., between the  $\{11.0\}$  MnAs and the  $\{110\}$  GaAs planes, is then only about 7.5%. First, we start with investigating the accommodation process originating from the 30% lattice misfit. The HRTEM micrograph in Fig. 2(a) reveals the interface character along the GaAs  $[110]$  projection. The HRTEM contrast of the MnAs lattice imaged in the  $[11.0]$  direction is wavy-like with a period corresponding to the hexagonal lattice constant  $c$  in agreement with HRTEM image simulations. Because of the different interference pattern on both sides, the interface can be determined very accurately and appears atomically abrupt in this projection. No localized misfit dislocation or strong coherence strain features, respectively, are visible in the HRTEM image. Therefore, at a first

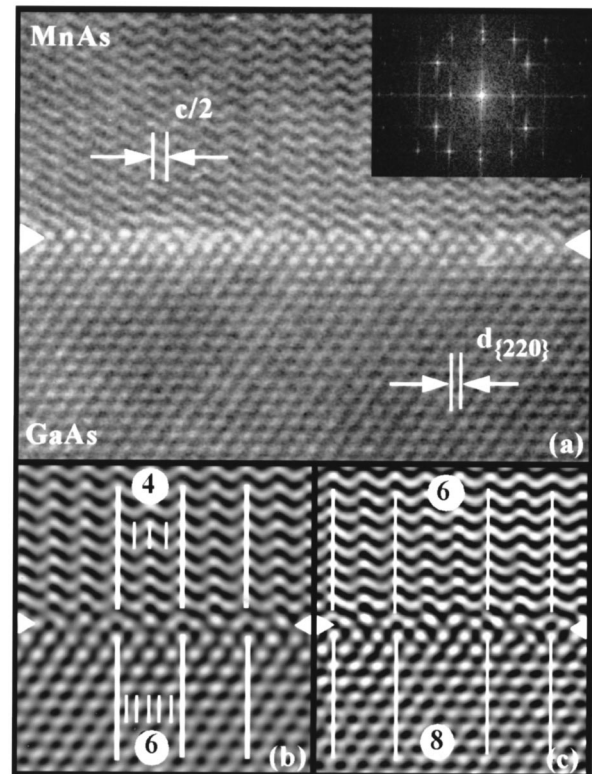


FIG. 2. Cross-sectional HRTEM image of the MnAs/GaAs interface in the MnAs  $[11.0] \parallel$  GaAs  $[110]$  projection. (a) Overview with an inset showing the Fourier power spectrum, (b) magnified part of the commensurate interface (after Fourier filtering), and (c) a coincidence lattice-misfit dislocation.

glance, the interface appears completely incoherent, as one would expect for heterosystems with large lattice mismatch and weak interfacial bond strength. However, a more careful inspection reveals an interface structure where the mismatch accommodation becomes understandable in the framework of a near-coincidence lattice model: every fourth  $\{00.2\}$  MnAs plane fits every sixth  $\{220\}$  GaAs plane forming a commensurate interface region [see Fig. 2(b)]. This 4/6 ratio reduces the natural lattice mismatch  $f$  from 30% to about 5%, a reasonable value to enable epitaxial growth. The deviation  $F$  from the exact coincidence, which is given by  $F = (4d_{\text{MnAs}}^{\{00.2\}} - 6d_{\text{GaAs}}^{\{220\}})/6d_{\text{GaAs}}^{\{220\}}$ , is accommodated by secondary defects related to the coincidence lattice, an example is shown in Fig. 2(c). Such defects are characterized by two additional  $\{00.2\}$  planes in one coincidence lattice mesh. The measured average spacing of these secondary defects at every third unit is sufficient to relieve the coincidence lattice misfit  $F$ , i.e., there is no residual strain detected in the  $[00.1]$  direction. In agreement with this result, the spacing of the reflections in the Fourier spectrum [inset in Fig. 2(a)] agrees with the strain-free bulk values. Thus, the resulting relaxed interface structure is composed of commensurate domains having perfect coincidence arrangement, which are separated by extended secondary dislocations.

In the following, we analyze the atomic interface structure along the lower misfit direction (7.5% misfit). Figure 3(a) shows a cross-sectional dark-field micrograph near the interface region imaged along the  $[00.1]$  MnAs  $\parallel$   $[1\bar{1}0]$  GaAs direction. The abrupt change in contrast evidences again the already mentioned smooth and chemically sharp boundary with no indication of an extended interfacial reaction zone. A

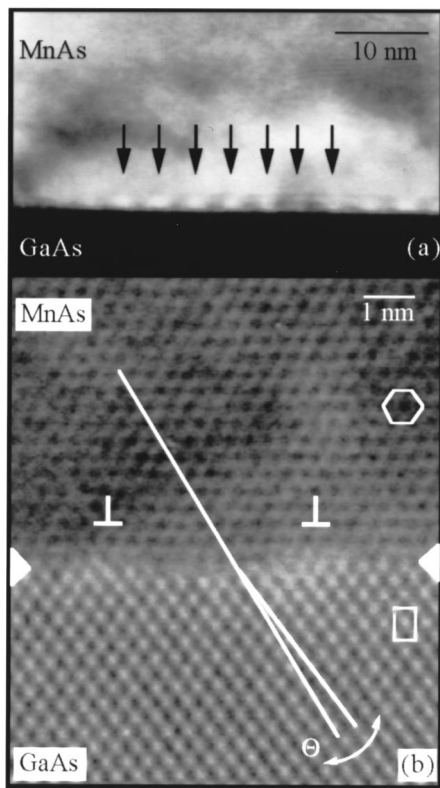


FIG. 3. Cross-sectional dark-field micrograph (a) and the HRTEM image (b) of the MnAs/GaAs interface with the incident beam parallel to MnAs[00.1]||GaAs[1 $\bar{1}$ 0]. Note the array of periodic strain contrast along the interface (arrows) in (a) and the lattice plane distortion in (b).

periodic array of strain contrast features along the interface is clearly observed, which is expected for an array of localized misfit dislocations. In fact, the HRTEM image in Fig. 3(b) confirms the semicoherent description of the interface where regions of perfect lattice matching are separated by misfit dislocations, which are characterized by a strong lattice plane bending perpendicular to the interface. The Burgers vector is determined to be  $\mathbf{b} = 1/3[11.0]$ , i.e., it is located parallel to the boundary plane and, therefore, most efficient in misfit strain relief. However, by measuring the mean distance  $\bar{D}$  between the dislocations,  $\bar{D} = (4.5 \pm 0.5)$  nm, a residual strain  $\epsilon^i$  in the epilayers at room temperature is calculated by applying the equation  $\epsilon_0^i = f_0^i - b^i/\bar{D}$ , where  $f_0^i$  defines the above introduced natural lattice misfit and  $b_i$  the in-plane Burgers vector component. Assuming that the mismatch between the MnAs layer and the GaAs substrate is completely relaxed at the growth temperature,<sup>8</sup> a residual compressive strain arises during sample cooling to room temperature, mainly because of a discontinuous increase of the lattice constant  $a$  of about 1% at the structural transition temperature  $T_c \approx 45$  °C.<sup>3</sup> This increase in the MnAs lattice constant is expected to decrease the lattice-mismatch value and, thus, is expected to increase the distance of the misfit dislocations. However, because of the relatively low temperature of the structural transition, the dislocations should be immobile to follow this change in the lattice constant, resulting in residual epilayer strain. In fact, this compressive stress state caused by the too closely spaced misfit dislocations is also verified by local lattice distortions in perfectly matched interfacial regions. In the HRTEM image [Fig. 3(b)], the angle  $\Theta$  between the misaligned  $\{111\}$  GaAs and  $\{1\bar{1}.0\}$  MnAs

planes increases from the unstressed value of  $5.26^\circ$  to  $6.5^\circ \pm 0.5^\circ$ , corresponding to a compressively stressed state in agreement with the results of the SAD pattern and the measured dislocation distance. The anisotropic residual strain must be, therefore, a result of the different misfit dislocation mobility  $v$  given by

$$v = v_0 \tau^m e^{-U(\tau)/(kT)}.$$

$U(\tau)$  is the energy barrier and depends on the applied shear stress  $\tau$  ( $v_0, m$  are constants). By assuming the Peierls–Nabarro (PN) model,<sup>9</sup> the shear stress  $\tau_{PN}$  for activating dislocation glide is proportional to the interfacial shear modulus  $G$  and depends on the dislocation core width  $w$

$$\tau_{PN} = 2G/Ke^{-2\pi w/(Kb)},$$

where the constant  $K$  represents the dislocation type. Therefore, the critical shear stress is certainly higher in the case of localized lattice dislocations compared to extended coincidence lattice dislocations having smaller  $G$  and larger  $w$  values. In addition, there is no large gap in the lattice constant  $c$  at  $T_c$  and, thus, in  $f^2$  resulting in a smaller  $\tau$ , we can, therefore, assume that the atomic arrangement along this interface direction can follow the stress evolution during cooling.

Despite this relative large amount of residual strain along the  $[1\bar{1}.0]$  direction, which also represents the easy-magnetization axis, the MnAs layers show, nevertheless, a high saturation magnetization value,<sup>6</sup> which is even higher than that of polycrystalline bulk MnAs. We can conclude from our investigation that the interplay between epitaxial strain and phase-transition-induced strain depends on the respective plastic relaxation mode: If the lattice misfit is completely relaxed during growth and the misfit dislocations are mobile until reaching  $T_c$ , the magnetic transition will not be affected by the epitaxial constraint, also, if the dislocations cannot follow the discontinuous volume change at  $T_c$ . On the other hand, an influence is expected if the misfit dislocations are immobile, i.e., in the case of an incomplete plastically relaxed epilayer.

In conclusion, we have demonstrated that the differences in crystal symmetry and lattice constants result in an anisotropic lattice-mismatch accommodation and, thus, in an anisotropic residual strain state. The residual strain is based on the different types of misfit dislocations and their different mobilities during the structural phase transition at  $T_c$ .

The authors would like to thank the Forschungszentrum Jülich, Institut für Festkörperforschung, for providing their microscope facilities.

<sup>1</sup>X. W. Li, A. Gupta, and G. Xiao, Appl. Phys. Lett. **75**, 713 (1999).

<sup>2</sup>Q. Gan, R. A. Rao, C. B. Eom, J. L. Garrett, and M. Lee, Appl. Phys. Lett. **72**, 978 (1998).

<sup>3</sup>B. T. M. Willis and H. P. Rooksby, Proc. Phys. Soc. London, Sect. B **67**, 290 (1954).

<sup>4</sup>C. P. Bean and D. S. Rodbell, Phys. Rev. **126**, 104 (1962).

<sup>5</sup>V. A. Chernenko, L. Wee, P. G. McCormick, and R. Street, J. Appl. Phys. **85**, 7833 (1999).

<sup>6</sup>F. Schippan, A. Trampert, L. Däweritz, K. H. Ploog, B. Dennis, K. U. Neumann, and K. R. A. Ziebeck, J. Cryst. Growth **201/202**, 674 (1999).

<sup>7</sup>Powder Diffraction File, ICDD, Swarthsmoor, PA, No. PDF 280644.

<sup>8</sup>This assumption is based on the fact that we have measured no thickness-dependent dislocation distance (residual strain) in samples with layer thickness between 2 and 150 nm.

<sup>9</sup>D. Hull and D. J. Bacon, *Introduction to Dislocations* (Pergamon, Oxford, UK, 1984).